JOURNAL OF PROPULSION AND POWER
Vol. 20, No. 5, September–October 2004

Frequency Veering Effects on Mistuned Bladed Disk Forced Response

J. A. Kenyon*
U.S. Air Force Research Laboratory, Wright–Patterson Air Force Base, Ohio 45433-7251
and
J. H. Griffin† and N. E. Kim‡
Carnegie Mellon University, Pittsburgh, Pennsylvania 15213

Bladed disk mistuning is a significant contributor to gas-turbine high cycle fatigue. Frequency veering is known to increase bladed disk sensitivity to mistuning, but the reasons for the increased sensitivity are not well understood. The frequency veering effects on mistuned bladed disk forced response are investigated. Expressions for the forced response of a mistuned bladed disk with frequency veering are developed. These expressions are cast in a form that identifies the mechanisms through which frequency veering affects mistuned forced response. The accuracy of these expressions is then demonstrated by the use of two numerical examples. The first example allows for the direct observation of frequency veering effects on mistuned response. The second example demonstrates the applicability of the theoretical development to realistic bladed disk models.

Nomenclature

$\boldsymbol{B}$	=	mode projection
$\boldsymbol{C}$	=	damping matrix
c	=	modal damping
E	=	engine order of excitation
F	=	generalized force
$\boldsymbol{f}$	=	forcing vector
j	=	bladed disk sector
$\boldsymbol{K}$	=	stiffness matrix
k	=	lumped stiffness or modal stiffness
$\boldsymbol{M}$	=	mass matrix
m	=	lumped mass or modal mass
N	=	number of blades
n	=	nodal diameter
r	=	tuned modal displacement ratio
t	=	time
x	=	displacement
β	=	mode participation factor
γ	=	proportionality constant
δ	=	Kronecker delta
δm	=	mass mistuning
ζ	=	modal damping ratio
η	=	scaling factor
θ	=	sector angle
$\boldsymbol{\Phi}$	=	mode shape matrix
ϕ	=	system mode shape
ψ	=	tuned sector mode shape
$\boldsymbol{\Omega}$	=	diagonal natural frequency matrix
ω	=	frequency

Subscripts

E	=	reference tuned mode
M	=	mistuned mode
p	=	mode index
q	=	mode index
V	=	veering tuned mode

Superscripts

C	=	cosine component
H	=	Hermitian operator
S	=	sine component
T	=	transpose operator
$\circ$	=	tuned

I. Introduction

MISTUNING of turbine engine bladed disks can lead to excessive blade vibration amplitudes that contribute to engine high cycle fatigue. Bladed disks are typically designed to be cyclically symmetric, so that each blade and its associated sector in the disk or hub are identical. Mistuning refers to small variations in the properties of the blade and disk sectors, which cause a breakdown in the cyclic symmetry. Bladed disks are quite sensitive to mistuning, and so even small variations in the blade and disk properties can lead to significant changes in forced response characteristics.

A significant research effort has been devoted to mistuning. Srinivasan[1] provides a good review of much of the early literature, particularly the development of statistical models. These models typically comprised lumped mass and stiffness parameters and were sometimes correlated with real engine data. More recent efforts have focused on modeling bladed disks with realistic geometry. These models are finite element based and can, thus, become computationally expensive, especially for statistical analyses. To alleviate the computational expense of finite element modeling, reduced-order modeling techniques have been developed. Castanier et al.[2] introduced a reduced-order method based on component mode synthesis. Here, the blades and disk are modeled separately, and the modes from the separate systems are superimposed. Yang and Griffin[3] later developed a method that computes the mistuned modes as a linear combination of the tuned modes. The Castanier et al. model was modified to include a similar formulation.[4,5] Petrov et al.[6] recently described a method that computes the mistuned response as a linear combination of tuned response transfer functions, a variation of the approach of Yang and Griffin.[3]

Received 13 June 2003; presented as Paper 2003-4976 at the AIAA/ASME/SAE/ASEE 39th Joint Propulsion Conference and Exhibit, Huntsville, Alabama, 20 July 2003; revision received 24 December 2003; accepted for publication 24 December 2003.

*Aerospace Engineer, Propulsion Directorate, 1950 Fifth Street. Member AIAA.
†William J. Brown Professor, Department of Mechanical Engineering, 5000 Forbes Avenue.
‡Senior Researcher, Department of Mechanical Engineering, 5000 Forbes Avenue.

Modeling of realistic modern bladed disk geometries resulted in the observation of frequency veering in tuned bladed disk system dynamics.[7] Frequency veering refers to the loci of the eigenvalues, for example, natural frequencies, of a dynamic system converging and then veering apart without crossing when the eigenvalues are plotted as a function of some physical parameter. Frequency veering occurs in a number of different types of structural dynamic systems and is generally associated with interaction between the system vibration modes.[8,9] In bladed disks, the frequency veering phenomenon has been observed in conjunction with rotor speed,[10,11] as well as interblade phase angle or nodal diameter.[2,7] The latter case is of interest in this paper. Modern bladed disks are particularly susceptible to frequency veering as a result of low aspect ratio blading. Low aspect ratio blades tend to compress more vibration modes into a smaller frequency space, leading to increased opportunities for mode interaction and, consequently, more numerous frequency veerings.

Frequency veering in bladed disks that occurs in conjunction with interblade phase angle or nodal diameter often involves interaction between blade-dominated and disk-dominated families of modes. The strain energy in the modes of a blade-dominated family tends to be concentrated in the blades, so that the number of nodal diameters in each mode has only a small effect on natural frequency. Consequently, the frequency locus appears nearly horizontal when plotted as a function of nodal diameter. In the disk-dominated family of modes, most of the strain energy resides in the disk, so that the number of nodal diameters in a mode shape can have a significant impact on the mode's natural frequency. Because a higher number of nodal diameters tends to increase the strain energy and, therefore, the frequency of a mode, the frequencies of a disk-dominated family appear to increase at a more rapid rate when plotted vs nodal diameter. When the frequency loci of the blade-dominated and disk-dominated families of modes converge, the mode families interact and frequency veering occurs.

Several studies of mistuned bladed disk response have indicated that frequency veering in the tuned system often results in increased sensitivity to mistuning and large mistuned response amplitudes.[2,7] It has been shown that frequency veering is related to coupling between mode shapes and that, in the presence of disorder, this coupling can lead to mode localization.[12] In a bladed disk, the interaction between the blade-dominated mode family and the disk-dominated mode family represents the coupling between mode shapes, and mistuning provides disorder. Mode localization in a bladed disk refers to the concentration of vibration energy in a small region of the bladed disk, resulting in large vibration amplitudes in a single blade or small group of blades. Localization is often cited as a leading cause of high-amplitude response and blade failure in mistuned bladed disks.[13]

Recently, Kenyon et al.[14] indicated that mode localization alone is not sufficient for extremely high blade vibration amplitudes. Instead, high response amplitudes occur when a balance is achieved between localization in the mode shape and a harmonic component in the mode that produces a large generalized force. The large generalized force is necessary to excite the mode with large amplitude, whereas the localization concentrates the vibration energy in a single blade or a few blades. Rivas-Guerra and Mignolet[15] corroborated this result. In this light, it is desirable to investigate more thoroughly the effects of frequency veering on mistuned forced response amplitudes to determine precisely why frequency veering leads to increased sensitivity to mistuning and increased forced response amplitudes.

This paper investigates the physics of mistuned forced response when frequency veering exists in the tuned system dynamics. Expressions are derived for the forced response of a mistuned bladed disk with frequency veering. These expressions are cast in a form that elucidates the physical mechanisms associated with frequency veering and how these mechanisms affect mistuned forced response. The accuracy of the expressions is then demonstrated with two numerical examples. The purpose of the examples is to corroborate the expressions and illustrate the role of the various mechanisms in actual cases. The first numerical example consists of a simple lumped parameter model with three degrees of freedom per sector. This type of model allows for the interaction between multiple families of modes, but is simple enough to perform Monte Carlo simulations to investigate the accuracy of the theoretical expressions. The second numerical example consists of a finite element bladed disk model with tapered blades. It illustrates that the same mechanisms are equally active in more realistic bladed disk geometries.

II. Theoretical Development

A. General Formulation

The equations of motion for the forced response of a bladed disk can be written in matrix form,

$$\boldsymbol{M}\ddot{\boldsymbol{x}} + \boldsymbol{C}\dot{\boldsymbol{x}} + \boldsymbol{K}\boldsymbol{x} = \boldsymbol{f}(t) \tag{1}$$

where $\boldsymbol{f}$ is an oscillatory force. For the tuned system, the modes are determined from the tuned eigenvalue problem

$$\boldsymbol{K}^{\circ}\boldsymbol{\Phi}^{\circ} = \boldsymbol{M}^{\circ}\boldsymbol{\Phi}^{\circ}\boldsymbol{\Omega}^{\circ 2} \tag{2}$$

In practice, the tuned modes of a bladed disk are determined by the use of a cyclic symmetry analysis.[16] The tuned sector modes ψ_n are calculated for a single sector with cyclic symmetry constraints at the sector boundaries, representative of the number of nodal diameters n in the bladed disk system modes, where $n = 0, 1, \ldots, N/2$ for N even or $n = 0, 1, \ldots, (N-1)/2$ for N odd. (Note that in the gas-turbine industry the term nodal diameter is commonly used to indicate the phase angle of the cyclic symmetric constraint applied in a single sector finite element analysis used to calculate the natural frequencies and mode shapes of the bladed disk. It is understood that the actual number of nodal diameters is often larger than this because of nodal diameters within the sector model; for example, torsion modes have at least one nodal diameter per blade.) The sector modes are normalized, so that the sector modal mass is unity. The tuned sector modes are then projected to the remainder of the disk. It is well-known that tuned bladed disks exhibit repeated natural frequencies for each n except $n = 0$, and, in the case of N even, $n = N/2$. For convenience, the tuned mode pairs are expressed here in real, that is, sine and cosine, form by the projection of a single sector mode shape ψ_n onto the jth sector, so that

$$\boldsymbol{\phi}_n^{\circ(j)C} = \psi_n \cos n\theta_j \tag{3}$$

$$\boldsymbol{\phi}_n^{\circ(j)S} = \psi_n \sin n\theta_j \tag{4}$$

where $\theta_j = 2\pi j/N$. For $n = 0$ or $N/2$, the bladed disk system mode is the single cosine mode, Eq. (3). In simple models where all of the degrees of freedom in a sector are described by the same annular coordinate, the degrees of freedom are either in phase or 180 deg out of phase within the sector, and this projection is straightforward. For more realistic cyclic symmetric finite element models, the continuity of the structure at the cyclic boundaries, as well as various characteristic blade and sector mode shapes, require that there may be a range of phase relations between degrees of freedom at different annular coordinates in the same sector. In this case, the relative motion of degrees of freedom within a sector are captured by the sector mode shape ψ_n, whereas the projection in Eqs. (3) and (4) relate a single degree of freedom, for example blade leading-edge tip in a sector to the equivalent degree of freedom in other sectors on the bladed disk. The projections of the tuned modes in Eqs. (3) and (4) preserve the orthogonality of the modes with respect to the tuned mass and stiffness matrices, so that

$$\boldsymbol{\phi}_p^{\circ T}\boldsymbol{M}^{\circ}\boldsymbol{\phi}_q^{\circ} = m_p\delta_{pq} \tag{5}$$

$$\boldsymbol{\phi}_p^{\circ T}\boldsymbol{K}^{\circ}\boldsymbol{\phi}_q^{\circ} = k_p\delta_{pq} \tag{6}$$

In addition, it is assumed that $\boldsymbol{C}$ may be expressed as a linear combination of the tuned mass and stiffness matrices. Consequently, the tuned modes are also orthogonal with respect to the damping matrix,

$$\boldsymbol{\phi}_p^{\circ T}\boldsymbol{C}\boldsymbol{\phi}_q^{\circ} = c_p\delta_{pq} \tag{7}$$

The forced response of the tuned bladed disk to an engine order traveling wave excitation is considered. The traveling wave describes the excitation that a rotor would experience as it rotates through stationary disturbances in the flow, such as wakes from upstream stator vanes. Because of the periodicity of the annulus, the disturbances can be Fourier decomposed spatially into wavelike forms with integer E harmonics. The excitation is described mathematically in a manner similar to the mode shapes. It consists of a sector distribution $\boldsymbol{f}_{\text{sector}}$, similar to a pressure distribution on a blade, that is projected in time and space to create a traveling wave of engine order E so that

$$\boldsymbol{f}(\theta_j, t) = \boldsymbol{f}_{\text{sector}} \cos(\omega t - E\theta_j) \tag{8}$$

In a tuned bladed disk, it is well-known that each blade or sector responds with the same amplitude,

$$\boldsymbol{x}_{\text{tuned}} = F_E \boldsymbol{\psi}_E / c_E \omega_E \tag{9}$$

where ω_E denotes natural frequency in the Eth tuned mode, $F_E = \eta \boldsymbol{\psi}_E^T \boldsymbol{f}_{\text{sector}}$, and $\eta = N/2$ for $E \notin \{N/2,\ N\}$ or $\eta = N$ for $E \in \{N/2,\ N\}$. Note that the E subscript refers to a reference tuned mode with $n = E$ because orthogonality of the trigonometric functions in Eqs. (3), (4), and (8) require that this constraint be satisfied for $F_E \neq 0$. In a frequency veering, there are two or more tuned modes that satisfy this condition. Therefore, one of these modes is selected as the reference. For the remainder of this paper, the reference mode is the tuned mode in the veering with the lowest frequency unless otherwise noted.

It has been shown that a mistuned mode can be well-approximated by a linear combination of a subset of tuned system modes.[3] Therefore, a mistuned mode is selected and expressed as a linear combination of the tuned modes belonging to the mode families that interact through the veering,

$$\phi_M = \sum_p \beta_p \phi_p^\circ \tag{10}$$

Here, the mode participation term β_p describes the contribution of the pth tuned mode to the mistuned mode, and the summation index p can be taken over all of the modes in the families in the veering. The mode participation terms are normalized, so that the contribution from the reference tuned mode β_E is unity.

The forced response of the mistuned mode to the excitation in Eq. (8) is considered. In this computation, two important details must be noted. First, because multiple tuned modes in the frequency veering have nodal diameter content equal to the engine order of the excitation, each of these tuned modes can contribute to the generalized forced in the mistuned mode. Without loss of generality, the case where two families of modes interact in the frequency veering is considered. When the cosine tuned mode in the first (lowest frequency) family of modes is chosen as the reference mode, $\beta_E^C = 1$, the generalized force in the mistuned mode is written

$$F_M = F_E + \beta_E^S F_E + \beta_V^C F_V + \beta_V^S F_V \tag{11}$$

where the V subscript denotes the second tuned mode pair in the veering for which $n = E$. The generalized force in the second tuned mode pair is $F_V = \eta \boldsymbol{\psi}_V^T \boldsymbol{f}_{\text{sector}}$, with η defined as before.

The second aspect of the forced response calculation to be considered is that, given Eq. (7), each of the tuned mode components in Eq. (10) contributes to the damping in the mistuned mode, so that

$$c_M = \sum_p \beta_p^2 c_p \tag{12}$$

a result consistent with Ref. 14. The mistuned forced response of the bladed disk may now be expressed,

$$\boldsymbol{x}_{\text{mistuned}} = F_M \phi_M / c_M \omega_M \tag{13}$$

where ω_M is the natural frequency of the mistuned mode and F_M and c_M are given by Eqs. (11) and (12), respectively. Because the blades do not all respond with equal amplitude, the entire mode shape must be retained in Eq. (13).

Amplitude magnification factor is typically the key parameter used to indicate the severity of mistuning effects on bladed disk forced response. The amplitude magnification factor is the ratio of the maximum mistuned response amplitude to the tuned response amplitude and denotes the factor by which mistuning increases the response in a bladed disk. Amplitude magnification is considered here by division of Eq. (13) by Eq. (9). Because each degree of freedom in a bladed disk model will have a different displacement, this calculation must be performed for each degree of freedom. To facilitate discussion, a single degree of freedom is selected, for instance, the leading-edge tip of a particular blade, and the degree of freedom is labeled x. The amplitude of the displacement at the degree of freedom is calculated for the mistuned and the tuned systems, and the ratio of the amplitudes is computed. The resulting amplitude magnification factor is a series of ratios of pertinent dynamic parameters,

$$x_{\text{mistuned}}/x_{\text{tuned}} = (F_M/F_E)(\phi_M/\psi_E)(c_E/c_M)(\omega_E/\omega_M) \tag{14}$$

Here, ϕ_M is the modal displacement at the selected degree of freedom in the mistuned mode, and ψ_E is the modal displacement at that degree of freedom in the tuned mode. Because all of the blades respond equally in the tuned bladed disk, the sector modal response is sufficient to describe the tuned modal displacement.

B. Frequency Veering Effects

The expression in Eq. (14) can be used in conjunction with Eqs. (10–12) to predict the amplitude magnification of a mistuned bladed disk with frequency veering. However, the expression does not provide much insight into the dynamics involved in the response, specifically, the physical mechanisms associated with frequency veering that lead to increased sensitivity to mistuning and increased amplitude magnification factors. Therefore, it is useful to introduce additional simplifications that allow closer study of the dynamic effects of frequency veering. In particular, the expression in Eq. (14) will be simplified and cast in a form that can be compared to a previous result derived for a single family of modes, that is, no frequency veering.[14]

To be consistent with the result in Ref. 14, only the contributions of the cosine tuned modes are included in Eq. (10). Based on the results in Ref. 17, this may be accomplished by the use of a mistuning pattern that is symmetric about some reference blade, which is labeled as having the coordinate $\theta_j = 0$. In addition, the response of the blade at that location, $\theta_j = 0$, is considered, so that the cosine terms in the mode shapes become unity. With these two simplifications, the modal displacement ϕ_M in Eq. (14) can now be written as the sector modal displacement in the mistuned mode,

$$\phi_M = \sum_p \beta_p \psi_p \tag{15}$$

where p is summed only over the cosine tuned modes. Furthermore, the expression for the generalized force is simplified,

$$F_M = F_E + \beta_V F_V \tag{16}$$

The C superscript for the cosine mode has been dropped from the expression. The damping expression in Eq. (12) remains unchanged, except that the summation is taken only over the tuned cosine modes.

Two additional simplifications may be made to the amplitude magnification. First, it is assumed that $\omega_M = \omega_E$. This assumption is justified because the frequency of a mistuned mode is typically only slightly different from the frequency of its corresponding tuned mode. Furthermore, it is known and can be observed in Eq. (9) that significant changes in frequency cause artificial changes in forced response not generally associated with mistuning. Second, the ratio $r_p = \psi_p/\psi_E$ is defined. By the use of these simplifications, the amplitude magnification factor at a selected degree of freedom in the

sector $\theta_j = 0$ can be written

$$\frac{x_{\text{mistuned}}}{x_{\text{tuned}}} = \frac{1 + \sum_{p \neq E} \beta_p r_p}{1 + \sum_{p \neq E} \beta_p^2 (c_p / c_E)} \left(1 + \beta_V \frac{F_V}{F_E} \right) \tag{17}$$

The mechanisms through which frequency veering impacts mistuned response can be observed directly by comparison of the expression in Eq. (17) with a similar expression developed for a single family of modes.[14] The expression, Eq. (15) of Ref. 14, is recast here in a similar format to that used in Eq. (17). The modes in Ref. 14 are normalized, so that c_p is equal in all modes, thereby tracking damping variations in the mode coefficients and allowing the damping terms to be eliminated explicitly from the expression for amplitude magnification. Here, the modes are normalized to have the same coefficient, so that damping in the tuned modes remains explicit in the expression for amplitude magnification. Therefore, the amplitude magnification factor at $\theta_j = 0$ for an isolated family of modes, Eq. (15) of Ref. 14, is rewritten

$$\frac{x_{\text{mistuned}}}{x_{\text{tuned}}} = \frac{1 + \sum_{p \neq E} \beta_p}{1 + \sum_{p \neq E} \beta_p^2 (c_p / c_E)} \tag{18}$$

By comparison of the expressions in Eqs. (17) and (18), it can be seen that frequency veering impacts mistuned response in three ways:

1) The modal density in the frequency veering is higher, so that the number of tuned modes that can contribute to the mistuned response is higher. This is reflected mathematically by a different range of mode index p in the summation terms.

2) The tuned sector modes are not necessarily all the same in the system with frequency veering, as reflected by the term r_p. This has important implications for forced response. If a tuned mode exhibits a larger displacement at the reference degree of freedom than the reference tuned mode, then r_p is large and the pth tuned mode contributes significantly to the forced response. However, if the tuned mode has a small response at the reference degree of freedom, then r_p is small and the pth tuned mode contributes little to the mistuned forced response.

3) As indicated by Eq. (16) and by the last parenthetical term in Eq. (17), the generalized forced in the mistuned system can have contributions from two tuned modes. This can lead to a significantly larger generalized force and, therefore, a significantly higher mistuned response amplitude. In fact, if F_V is of the same order of magnitude as F_E, the mistuned forced response amplitude and the amplitude magnification factor may more than double due to the increased generalized force. In the case of $F_V \gg F_E$, the amplitude magnification factor of Eq. (17) may become extremely large.

C. Dual Tuned Modes

Another difference between forced response in an isolated family of modes and forced response in a frequency veering is that more than one tuned mode pair can respond to an engine order excitation in a frequency veering. The tuned forced response amplitude in the second mode pair is again the same for all blades and is given by

$$\boldsymbol{x}_{\text{tuned}} = F_V \boldsymbol{\psi}_V / c_V \omega_V \tag{19}$$

The amplitude magnification of the mistuned response with respect to the second tuned mode pair can be derived in the same way as described earlier, except that the second tuned mode pair is selected as the reference. In this case, Eq. (19) becomes Eq. (9), and the computation proceeds as before.

Note that it was pointed out in Sec. II.B. that in the case of $F_V \gg F_E$, the amplitude magnification may become extremely large. The large amplitude magnification is essentially the result of a small reference tuned response due to a small generalized force exciting the tuned modes. If the second tuned mode pair is instead taken as the reference, the inequality is reversed, $F_V \ll F_E$, and the contribution of the generalized force to the amplitude magnification factor is small, though the other effects of mistuning and frequency veering may lead to large amplitude magnification. In practice, the maximum forced response in either of the tuned mode pairs is taken as the reference, so that there is a practical limit on the amplitude magnification factor.

III. Numerical Demonstration

The expressions for amplitude magnification in a mistuned bladed disk with frequency veering are demonstrated numerically in this section. Two numerical examples are presented. The first example consists of a simple, lumped parameter model with three degrees of freedom per sector. A symmetric mistuning pattern is used in this example, so that the simplified expression for amplitude magnification at $\theta_j = 0$, Eq. (17), can be applied. In this way, this example can be used to discuss the effects of frequency veering on mistuned response in some detail. The second example consists of a finite element model of a bladed disk with tapered blades. This example is used to illustrate the more general expression of Eq. (14). Moreover, the second example demonstrates the applicability of the theoretical development to full bladed disk finite element models. It should be emphasized that the purpose of the numerical examples is to show that the expressions in Eqs. (14) and (17) capture the essential physics of mistuning in regions of frequency veering. The expressions then form the basis of a more complete understanding of the effects of frequency veering on mistuned bladed disk forced response.

A. Lumped Parameter Example

The first numerical example consists of a lumped parameter bladed disk model with three degrees of freedom per sector (Fig. 1). The sectors are connected cyclically via the coupling springs k_c, so that $\theta_{j=N} = \theta_{j=0}$. For purposes of discussion, the degrees of freedom corresponding to m_1 and m_2 will be referred to as blade degrees of freedom, whereas the motion of m_3 will be referred to as a disk degree of freedom because it is coupled to adjacent sectors by the use of cyclic constraints, as represented by k_c. The beamlike elements between masses represent linear springs that deflect laterally. The model bladed disk has 10 blades, and the nominal system parameters for the model are given in Table 1. These system parameters result in a frequency veering in the second and third families of modes near two nodal diameters (Fig. 2).

To study the effects of the frequency veering, the harmonic, steady-state response of the system to a second engine order excitation ($E = 2$) was calculated in an independent numerical forced response simulation. The sector forcing distribution was applied to the blade degrees of freedom, that is, $\boldsymbol{f}_{\text{sector}} = [1 \;\; 1 \;\; 0]^T$. The tuned forced response amplitude of the bladed disk model was calculated, with the frequency resolution selected for the forced response

Table 1 Lumped parameters for simple model

Parameter	Value
m_1	12
m_2	8
m_3	27
k_1	52
k_2	6
k_3	230
k_c	51

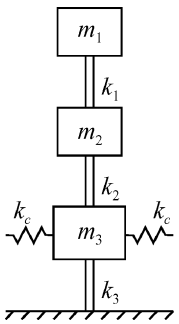

Fig. 1 Lumped parameter bladed disk model.

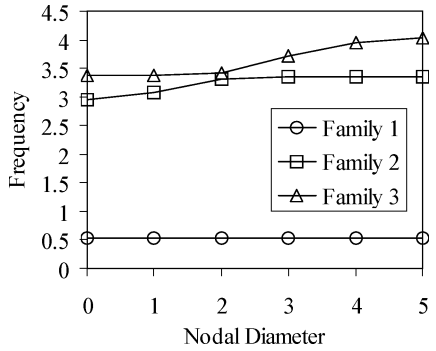

Fig. 2 Frequencies vs nodal diameters for lumped parameter model.

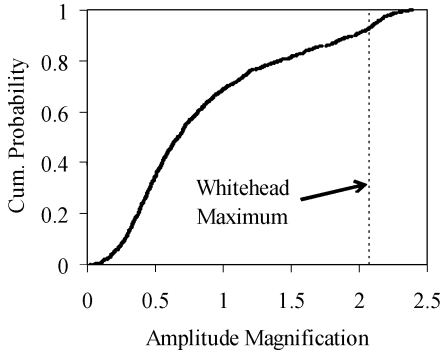

Fig. 3 Cumulative probability distribution of mistuned amplitude magnification with frequency veering.

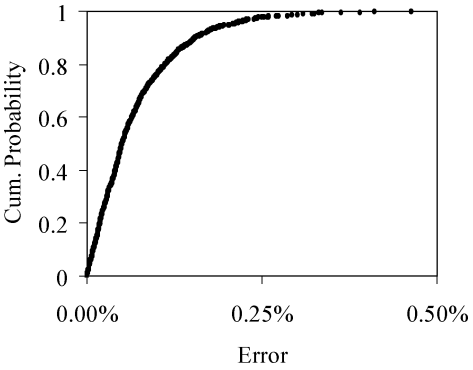

Fig. 4 Cumulative probability distribution of error in theoretical prediction for lumped parameter model.

simulation to provide less than 0.1% error in the response amplitude. Monte Carlo simulations were then performed to observe the accuracy of Eq. (17) for a large number of mistuned bladed disks. The expression for amplitude magnification factor in Eq. (17) requires that the mistuned mode consist of only cosine components. Therefore, only mistuning patterns that were symmetric about a reference blade at $\theta_j = 0$ were considered for this example.[17] For the Monte Carlo simulations, a random mistuning pattern was generated and applied to one-half of the bladed disk (six blades) and then projected symmetrically about a selected reference blade to the other half of the bladed disk. In other words, if $\theta_j = 0$ is at blade 1, then blade 2 had the same mistuning as blade 10, blade 3 had the same mistuning as blade 9, etc. The mistuning pattern in the first one-half of the disk consisted of normally distributed variations in the masses of the blade degrees of freedom with zero mean and a standard deviation of 2% of the nominal mass. The same percent variation was applied to both degrees of freedom in each sector.

The following procedure was used to determine a theoretical prediction of the results from Eq. (17): The reference mode was selected as the two-nodal diameter mode in family 2, Fig. 2. The modal displacement ratios r_p, modal damping c_p, and generalized forces F_E and F_V were then computed. Once the mistuning pattern was applied to the system and the system modes were determined for each Monte Carlo simulation, the mistuned modes were projected onto the tuned system modes to obtain the mode participation terms,

$$\boldsymbol{B} = \boldsymbol{\Phi}^{\circ -1}\boldsymbol{\Phi}_M \tag{20}$$

The columns of $\boldsymbol{B}$ represent the mode participation terms β_p for each mistuned mode. For the theoretical calculation, a mistuned mode was selected in which the reference tuned mode projection β_E was the largest tuned component in the mistuned mode. The mode participation terms in the selected mistuned mode were then normalized, so that $\beta_E = 1$, and these values of β_p were used in Eq. (17) to predict the amplitude magnification of the mistuned mode. Finally, because the mistuned frequencies in the Monte Carlo simulations were not constrained to be equal to the frequency of the reference mode, the expression in Eq. (17) was multiplied by ω_E/ω_M. [See Eq. (14).]

The numerical forced response simulation was then performed to determine independently the forced response of the selected mistuned mode. Small damping levels were used in the numerical simulation to isolate the response of individual modes. From a practical standpoint, the damping values used in the numerical simulations were smaller than would normally be observed in a bladed disk. However, because the goal of this paper is to investigate how frequency veering affects individual modes and the forced response of the system in those modes, it is useful to employ small damping to isolate individual resonant peaks and study the response of the system in a mode corresponding to a single resonant peak. Again, the frequency resolution was selected for the forced response simulation to provide less than 0.1% error in the response amplitude. In this way, the response in the selected mistuned mode was calculated and divided by the tuned response amplitude to obtain the amplitude magnification factor. The amplitude magnification factor from the forced response simulation was then compared to the theoretical prediction.

This process was repeated for a total of 1000 Monte Carlo simulations. The cumulative probability distribution for the amplitude magnification factor at m_1 is shown in Fig. 3. The cumulative probability distribution represents the probability (ordinate) that the amplitude magnification will be at or below the corresponding value on the abscissa. Two observations can be made from Fig. 3. First, there is a large variation in the amplitude magnification, indicating that the response is very sensitive to mistuning. Second, there is a significant probability of an extremely high amplitude magnification factor in the mistuned response with frequency veering. As a reference, the maximum amplitude magnification predicted by Whitehead[18] is shown by a line on the chart. The results from the Monte Carlo simulation indicate that, with the frequency veering, there is approximately a 7% chance that this maximum will be exceeded, even though only relatively small mistuning is used. Again, this probability is only for the reference blade in the selected mistuned mode. Therefore, the actual probability of the bladed disk exceeding this maximum is even higher.

The most significant result from the Monte Carlo simulations is the agreement between the theoretical predictions and the numerical result. The cumulative probability distribution of the error in the theoretical prediction is given in Fig. 4. The percent error is computed as

$$\text{Error} = \frac{\text{Theory} - \text{Simulation}}{\text{Simulation}} \times 100\% \tag{21}$$

As shown in Fig. 4, the maximum error over 1000 simulations was less than 0.5%. The largest errors tended to occur when the amplitude magnification was small. In these cases, the small differences between the theoretical predictions and numerical results were exacerbated by the fact that the predictions and numerical results were also small numbers, thereby creating the appearance of more significant errors and the tail behavior observed in Fig. 4. The results in Fig. 4 indicate that the expression for the amplitude magnification in

Table 2 Blade mistuning for lumped parameter model

Blade	δm, %
1	3.09
2	0.34
3	1.60
4	−3.41
5	0.35
6	−0.96
7	0.35
8	−3.41
9	1.60
10	0.34

Table 3 Mistuned mode projections onto tuned mode

Mode	β_0	β_1	β_2	β_3	β_4	β_5
Family 2	−0.004	−0.016	1.000	0.584	0.342	0.110
Family 3	0.134	0.281	0.145	0.010	0.002	0.001

Eq. (17) accurately represents the forced response amplitude magnification factor in a mistuned bladed disk with frequency veering.

To more closely investigate the effects of frequency veering on mistuned bladed disk forced response, one of the simulations from the Monte Carlo study was singled out for more detailed examination. The specific example consists of one of the cases that resulted in response greater than the limit proposed by Whitehead.[18] The blade mass mistuning δm in this example is given in Table 2. It is clear from table 2 that the mistuning pattern is symmetric about blade 1, meaning that blade 1 corresponds to the location $\theta_j = 0$. The blade mistuning was applied, and the mistuned modes were computed. A mistuned mode was selected as described earlier and projected onto the tuned system modes to obtain the mode participation terms β_p. These are provided in Table 3. Only the cosine mode participation terms are shown because $\beta_p = 0$ for all of the sine modes. The mode participation terms are listed by mode family, and then by the number of nodal diameters in the mode shape, to facilitate discussion. Note that the largest values of β_p occur in the tuned modes with frequencies nearest the reference tuned mode, β_2 of family 2 (Fig. 2). This is consistent with Yang and Griffin's result.[19] They found that the strongest participation in a mode interaction due to a perturbation such as mistuning comes from the unperturbed (tuned) modes with frequencies nearest the perturbed (mistuned) mode of interest.[19] The mode participation terms from family 1 are not shown in Table 3 because these tuned modes did not participate in the mistuned response.

For this forced response simulation, the damping matrix was $\boldsymbol{C} = 0.0015\boldsymbol{M}^{\circ} + 0.0001\boldsymbol{K}^{\circ}$, resulting in a damping ratio $\zeta \approx 0.04\%$ in the tuned and mistuned modes. The amplitude magnification factor was predicted by the use of Eq. (17) and the appropriate parameters from the tuned system analysis. A numerical forced response simulation was then performed. The results are shown in Fig. 5. Here, the frequency response functions are normalized by the maximum tuned response amplitude, so that the results are presented as amplitude magnification. As shown in Fig. 5, the predicted amplitude magnification agrees very well with the numerical result.

The extremely large amplitude magnification factor shown in Fig. 5 can be attributed directly to the effects of frequency veering on mistuned forced response. As pointed out in Sec. II.B, frequency veering impacts mistuned amplitude magnification in three ways. The increase in modal density is not a major factor in the amplitude magnification of this particular example because only the modes with frequencies near the tuned reference frequency participate significantly (Table 3 and Fig. 2). However, the increase in generalized force from the frequency veering is sizeable. When $F_E = \eta \psi_E^T \boldsymbol{f}_{\text{sector}}$ and $F_V = \eta \psi_V^T \boldsymbol{f}_{\text{sector}}$ are computed from the tuned system modes and the prescribed forcing vector, the ratio $F_V/F_E = 1.10$. When multiplied by β_V according to Eq. (17), or, equivalently, by β_2 from family 3 in Table 3, the additional generalized force results in an increase of approximately 16% in mistuned forced response amplitude. In other words, the amplitude magnification would have been approximately 1.86 without the increased generalized force, instead of the value 2.16 shown in Fig. 5. More important than the increased generalized force for this example are the relative motion effects from the tuned modes near the frequency veering. The values of the modal displacement ratios r_p are shown in Table 4 for the families of modes interacting in the frequency veering. By comparison of Table 4 to the mode contribution terms in Table 3, it is clear that the tuned modes contributing most significantly to the mistuned response also exhibit modal displacement ratios greater than one. In terms of forced response, this means that these tuned modes contribute very strongly to the mistuned response in the selected degree of freedom, leading to a high mistuned vibration amplitude.

Table 4 Modal displacement ratios for lumped parameter example

Mode	r_0	r_1	r_2	r_3	r_4	r_5
Family 2	0.21	0.27	1	1.31	1.32	1.32
Family 3	1.30	1.29	0.86	0.14	0.07	0.06

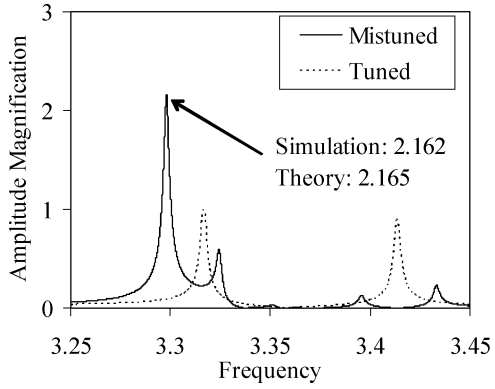

Fig. 5 Numerical forced response simulation for lumped parameter model.

The lumped parameter example described here demonstrates the accuracy of the expression in Eq. (17) for amplitude magnification. In addition, it illustrates how specific frequency veering mechanisms contribute to increased mistuned response: 1) Frequency veering leads to a substantial increase in generalized force. 2) The relative motion of the tuned modes near the frequency veering contributes to high amplitude mistuned response in the selected degree of freedom. Therefore, it is clear that Eq. (17) provides not only a means for predicting mistuned amplitude magnification with frequency veering, but also a useful tool for understanding how various frequency veering mechanisms affect mistuned forced response.

B. Finite Element Example

The second numerical example consists of a finite element model of a bladed disk with 18 tapered blades (Fig. 6). The natural frequencies are shown as a function of nodal diameter in Fig. 7. The mode families to be considered here are highlighted by the smaller box in Fig. 7, and the blade mode shapes in these mode families are displayed. Although a frequency veering is not apparent in Fig. 7, the blade mode shapes essentially exchange from zero nodal diameters to nine nodal diameters, indicative of mode interaction behavior consistent with frequency veering. Instead of disk and blade mode interaction, as is often observed with frequency veering, this example consists of interaction between two blade-dominated families of modes. The bladed disk was subjected to a fourth engine order ($E = 4$) traveling wave excitation consisting of a unit point force at each blade leading-edge tip.

The tuned modes of the bladed disk were determined, and the response of the four nodal diameter mode with the highest frequency was selected as the reference. Mistuning was modeled as a change in the elastic modulus of the bladed disk material in the blade elements forward of the blade midchord. In other words, the stiffness of the blade elements along the entire blade length from the midchord to the leading edge of each blade was varied, which effectively varied

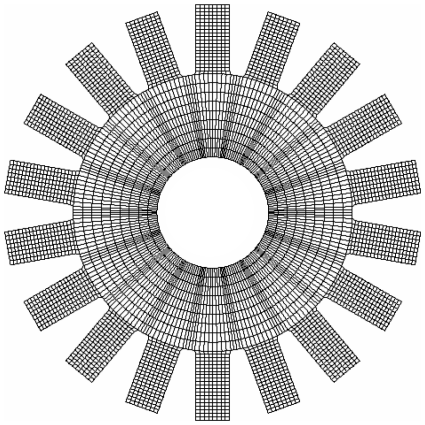

Fig. 6 Finite element bladed disk model with tapered blades.

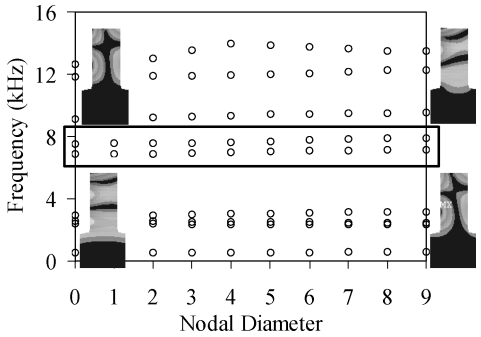

Fig. 7 Frequencies vs nodal diameters for finite element bladed disk model.

the blade stiffness, predominantly in the torsion-dominated modes. A random mistuning pattern was generated with a standard deviation of 9% in the elastic modulus or stiffness. The mistuning pattern was applied to the bladed disk, and the mistuned modes were calculated. A mistuned mode was selected with frequency near the reference tuned frequency, and the selected mode was projected onto the tuned modes [Eq. (20)] to determine the mode participation terms β_p. The modal displacement at the tip of each blade was then calculated for the mistuned mode by the use of Eq. (10). Note that the tuned modes from the finite element model were expressed in complex form, so that the mistuned mode projections β_p were also complex. In addition, both the tuned and mistuned modes were mass normalized so that the β_p terms are scaled differently from Sec. II. However, Eq. (10) still provides an accurate description of the mistuned mode. The maximum modal response occurred in blade 9 ($\theta = 160$ deg), and so the displacement at the leading-edge tip of blade 9 is used for discussion here. The generalized forces in the tuned system F_E and F_V were determined, and the generalized force in the selected mistuned mode F_M was calculated from Eq. (11). The mode participation terms and tuned generalized forces were recast in complex notation, corresponding to the finite element formulation. Finally, the damping matrix $\boldsymbol{C}$ was chosen to be proportional to the tuned mass matrix, $\boldsymbol{C} = \gamma \boldsymbol{M}^{\circ}$, with γ chosen so that $\zeta_E \approx \zeta_M = 1.92E^{-5}$. The small damping allows for consideration of a single mistuned mode in the forced response. The damping in the mistuned mode was calculated by the use of Eq. (12).

With all of the necessary parameters determined, the amplitude magnification in the selected mistuned mode was calculated from Eq. (14). The predicted amplitude magnification factor in blade 9 was 1.69. A forced response simulation was performed with the tuned and mistuned finite element models, with the frequency resolution selected so that the numerical error in each of the simulations was less than 0.25%. The mistuned response was divided by the tuned response to obtain the amplitude magnification from the simulations. The numerical amplitude magnification factor was 1.68, in good agreement with the theoretical prediction.

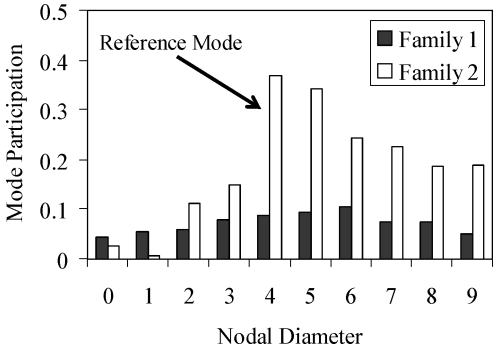

Fig. 8 Mode participation factors for finite element example.

The effects of frequency veering can be observed by consideration of each of the terms in Eq. (14). This expression consists of four ratios of important parameters that multiply together to form the mistuned amplitude magnification factor. For ease of discussion, each of these ratios is considered individually here, in reverse order from how they appear in Eq. (14), beginning with the frequency and modal damping ratios. It was found that these two ratios do not significantly impact the amplitude magnification for this example. The frequency of the tuned reference mode $\omega_E = 7644$ Hz, whereas the frequency of the mistuned mode of interest is $\omega_M = 7601$ Hz. Therefore, the ratio $\omega_E/\omega_M = 1.006$, near unity. The damping matrix was assumed to be proportional to the mass matrix, and the finite element modes were mass normalized, so that $c_p = c_E \; \forall \, p$. Accounting for the complex mode projections, the mistuned modal damping [Eq. (12)] becomes $c_M = c_E \boldsymbol{\beta}^H \boldsymbol{\beta}$, and the modal damping ratio $c_E/c_M = 1/\boldsymbol{\beta}^H \boldsymbol{\beta}$. Calculation of this ratio for the finite element example gives $c_E/c_M = 0.992$, also near unity. Because the natural frequency and modal damping ratios do not contribute significantly in Eq. (14) for this example, it is clear that the high amplitude magnification is primarily a result of the mistuned mode shape and generalized force.

The modal displacement ratio ϕ_M/ψ_E was the greatest contributor to the amplitude magnification factor, with $\phi_M/\psi_E = 4.252$ from the finite element results. To facilitate discussion, the amplitudes of the mode participation terms are shown in Fig. 8 as a function of nodal diameter and tuned mode family. It can be seen in Fig. 8 that most of the modes in both tuned mode families contribute significantly to the mistuned response. It was found that the tuned modal displacement ratios $|r_p|$ were approximately unity for the modes in family 2, whereas $|r_p|$ was approximately 0.8 for each of the modes in family 1. More importantly, the motion in each of these tuned modes at blade 9 was nearly in phase. Therefore, although the relative motion in the tuned modes is not a major factor in the response, the high modal density due to the frequency veering means that a large number of tuned modes contribute to the mistuned modal response at blade 9, leading to the high response in the mistuned mode.

The final ratio in Eq. (14) to be considered is the generalized force ratio, F_M/F_E. For this example, $F_M/F_E = 0.399$, indicating that the generalized force in the mistuned mode served to mitigate the amplitude magnification in the finite element model. It was found that the four nodal diameter mode in family 1 made only a small contribution to the mistuned generalized force, so that the effect of frequency veering on the generalized force was small. The reduction of generalized force in the mistuned mode comes about because the modal response and modal energy are spread over a number of harmonics that do not contribute to the generalized force. Because both the tuned reference mode and the mistuned mode are mass-normalized, the amplitude of the fourth harmonic in the normalized mode shape is less in the mistuned mode than it is in the tuned reference mode, resulting in a reduction in the generalized force in the mistuned bladed disk. The reduction in generalized force from the dispersion of modal energy is not clear in the development of Sec. II due to the mode normalization used in the derivation. However, it becomes clear when a consistent mass normalization is employed, as in this example. The tradeoff between modal response

and generalized force as observed in this example is discussed in Ref. 14.

This example demonstrates that the expression in Eq. (14) accurately predicts the amplitude magnification factor in the mistuned finite element bladed disk model. Because this expression captures the essential physical mechanisms associated with frequency veering and mistuned response described in Sec. II, it is clear from this example that these mechanisms are present in the response of realistic bladed disk models. For this example, the primary effect of frequency veering is increased modal density, which allows a large number of tuned modes to contribute to the mistuned response. The effects of frequency veering on tuned mode relative motion and generalized force affect the forced response in this example only to a small degree. By application of the expression in Eq. (14) to the finite element model in this example, the new insight gained from the expressions developed in Sec. II can be extended to the mistuned response of real bladed disks with frequency veering.

IV. Conclusions

Expressions for the amplitude magnification factor in a mistuned bladed disk with frequency veering are developed. These expressions are cast in a form that identifies the mechanisms through which frequency veering affects mistuned forced response. First, the modal density in the frequency veering is high, so that a large number of tuned modes can contribute to the mistuned response. Second, the sector mode shapes of the tuned system vary based on mode family and interblade phase angle. As a consequence, some tuned modes may exhibit a large response in a particular degree of freedom, whereas others may exhibit very low response in the same degree of freedom. If a number of tuned modes with a large response in a particular location contribute strongly to the mistuned response, then the resulting mistuned response at that location will be very large. The amplitude magnification factor is further exacerbated if the reference tuned mode exhibits relatively low response at that location on the bladed disk. Last, the generalized forced in the mistuned system can have contributions from more than one tuned mode. This can lead to a significantly larger generalized force exciting the mistuned system and, therefore, a significantly higher mistuned response amplitude.

The expressions for amplitude magnification are corroborated by the use of two numerical examples. The first example consists of a lumped parameter bladed disk model with three degrees of freedom per sector. Monte Carlo simulations were performed with this model, with the amplitude magnification from each numerical forced response simulation compared to the predicted amplitude magnification for the same mistuned bladed disk. Two important observations were made from the Monte Carlo simulations. First, the frequency veering led to a significant probability of extremely high amplitude magnification in the mistuned bladed disk. Second, and perhaps more importantly, excellent agreement between the predicted response and the numerical result was observed for all of the simulations, signifying the accuracy of the expressions derived here. One of the Monte Carlo simulations that exhibited a high amplitude magnification factor was selected for more detailed study. The effects of frequency veering described in the preceding paragraph were observed directly. In particular, the tuned modes that contributed strongly to the mistuned response exhibited large displacements in the selected degree of freedom, leading to a large vibration amplitude in the mistuned bladed disk. The generalized force in the mistuned system further increased the mistuned response amplitude significantly.

The second numerical example consisted of a finite element model of a bladed disk with tapered blades. Here, two blade-dominated families of modes interacted. The system was mistuned by variation of the stiffness of the elements forward of the mid-chord of each blade. The predicted amplitude magnification agreed with the results from a numerical forced response simulation, again showing the accuracy of the expressions derived here. In this example, the primary effect of frequency veering was increased modal density, which allowed a large number of tuned modes to participate in the mistuned response. By application of the expressions for amplitude magnification to a finite element model, this example allows the new insight into mistuned response with frequency veering to be extended to realistic bladed disk models.

References

[1]Srinivasan, A. V., "Flutter and Resonant Vibration Characteristics of Engine Blades," *Journal of Engineering for Gas Turbines and Power*, Vol. 119, No. 4, 1997, pp. 742–775.

[2]Castanier, M. P., Óttarsson, G., and Pierre, C., "A Reduced-Order Modeling Technique for Mistuned Bladed Disks," *Journal of Vibration and Acoustics*, Vol. 119, No. 3, 1997, pp. 439–447.

[3]Yang, M.-T., and Griffin, J. H., "A Reduced Order Model of Mistuning Using a Subset of Nominal System Modes," *Journal of Engineering for Gas Turbines and Power*, Vol. 123, No. 4, 2001, pp. 893–900.

[4]Bladh, R., Castanier, M. P., and Pierre, C., "Component-Mode-Based Reduced Order Modeling Techniques for Mistuned Bladed Disks–Part I: Theoretical Models," *Journal of Engineering for Gas Turbines and Power*, Vol. 123, No. 1, 2001, pp. 89–99.

[5]Bladh, R., Castanier, M. P., and Pierre, C., "Component-Mode-Based Reduced Order Modeling Techniques for Mistuned Bladed Disks–Part II: Application," *Journal of Engineering for Gas Turbines and Power*, Vol. 123, No. 1, 2001, pp. 100–108.

[6]Petrov, E. P., Sanliturk, K. Y., and Ewins, D. J., "A New Method for Dynamic Analysis of Mistuned Bladed Disks Based on the Exact Relationship Between Tuned and Mistuned Systems," *Journal of Engineering for Gas Turbines and Power*, Vol. 124, No. 3, 2002, pp. 586–597.

[7]Bladh, R., Pierre, C., Castanier, M. P., and Kruse, M. J., "Dynamic Response Predictions for a Mistuned Industrial Turbomachinery Rotor Using Reduced-Order Modeling," *Journal of Engineering for Gas Turbines and Power*, Vol. 124, No. 2, 2002, pp. 311–324.

[8]Perkins, N. C., and Mote, C. D., "Comments on Curve Veering in Eigenvalue Problems," *Journal of Sound and Vibration*, Vol. 106, No. 3, 1986, pp. 451–463.

[9]Balmés, E., "High Modal Density, Curve Veering, Localization: A Different Perspective on the Structural Response," *Journal of Sound and Vibration*, Vol. 161, No. 2, 1993, pp. 358–363.

[10]Kenyon, J. A., "Investigation of Curve Veering Using Computational and Experimental Techniques," *Proceedings of the 40th AIAA/ASME/ASCE/AHS/ASC Structures, Structural Dynamics, and Materials Conference*, Vol. 2, AIAA, Reston, VA, 1999, pp. 1550–1558.

[11]Marugabandhu, P., and Griffin, J. H., "A Reduced-Order Model for Evaluating the Effect of Rotational Speed on the Natural Frequencies and Mode Shapes of Blades," *Journal of Engineering for Gas Turbines and Power*, Vol. 125, No. 3, 2003, pp. 772–776.

[12]Pierre, C., "Mode Localization and Eigenvalue Loci Veering Phenomena in Disordered Structures," *Journal of Sound and Vibration*, Vol. 126, No. 3, 1988, pp. 485–502.

[13]Wei, S.-T., and Pierre, C., "Localization Phenomena in Mistuned Assemblies with Cyclic Symmetry Part II: Forced Vibrations," *Journal of Vibration, Acoustics, Stress, and Reliability in Design*, Vol. 110, No. 4, 1988, pp. 439–449.

[14]Kenyon, J. A., Griffin, J. H., and Feiner, D. M., "Maximum Bladed Disk Forced Response from Distortion of a Structural Mode," *Journal of Turbomachinery*, Vol. 125, No. 2, 2003, pp. 352–363.

[15]Rivas-Guerra, A. J., and Mignolet, M. P., "Maximum Amplification of Blade Response Due to Mistuning: Localization and Mode Shape Aspects of the Worst Disks," *Journal of Turbomachinery*, Vol. 125, No. 3, 2003, pp. 442–454.

[16]Thomas, D. L., "Dynamics of Rotationally Periodic Structures," *International Journal for Numerical Methods in Engineering*, Vol. 14, No. 1, 1979, pp. 81–102.

[17]Kenyon, J. A., and Griffin, J. H., "Forced Response of Turbine Engine Bladed Disks and Sensitivity to Harmonic Mistuning," *Journal of Engineering for Gas Turbines and Power*, Vol. 125, No. 1, 2003, pp. 113–120.

[18]Whitehead, D. S., "The Maximum Factor by Which Forced Vibration of Blades Can Increase Due to Mistuning," *Journal of Engineering for Gas Turbines and Power*, Vol. 120, No. 1, 1998, pp. 115–119.

[19]Yang, M.-T., and Griffin, J. H., "A Normalized Eigenvalue Approach for Resolving Modal Interaction," *Journal of Engineering for Gas Turbines and Power*, Vol. 119, No. 3, 1997, pp. 647–650.